SpartANN - Spectral Pattern Analysis and Remote-sensing Tool with Artificial Neural Networks

Marco Dinis[1,2], Pedro Tarroso[1,2]

1: CIBIO, Centro de Investigação em Biodiversidade e Recursos Genéticos, InBIO Laboratório Associado, Campus de Vairão, Universidade do Porto, 4485-661 Vairão, Portugal

2: BIOPOLIS Program in Genomics, Biodiversity and Land Planning, CIBIO, Campus de Vairão, 4485-661 Vairão, Portugal

Corresponding author: Marco Dinis (marco.dinis@cibio.up.pt; dinismarco6@gmail.com)

Abstract

Remote sensing, particularly from satellite observation, has become the standard tool for monitoring the planet with a steady increase of data production, and has seen wide application in ecosystem services analysis and management. Many remote sensing applications involve image classification, using methods from simple regressions to complex machine learning approaches that require advanced user expertise. Many approaches rely on a single model, which fails to account for the uncertainty inherent in the stochastic nature of single-model methods. This work introduces SpartANN – an open-source tool for image classification combining Artificial Neural Networks and ensemble modelling approaches, allowing users the flexibility to customize model parameters, identify areas of model congruence and quantify prediction uncertainty. We demonstrate the flexibility of SpartANN by performing a cloud-cover classification exercise on Sentinel-2 images and discuss the success of classification outputs and advantages of SpartANN.

Keywords:

Artificial Neural Networks; Cloud cover classification; Ensemble modelling; Open-source; python.

1. Introduction

The continuous influx of satellite imagery from multiple satellites, alongside data acquisition from novel techniques such as drones, offers both opportunities and challenges for research. Remotely sensed imagery has been increasingly utilized across a wide range of domains, including land cover mapping (Campos and Brito, 2018), wildfire monitoring and impact (Santos et al., 2022; Zhou et al., 2024), extreme weather and drought assessment (Kislov et al., 2021; Wang and Zhang, 2024), air quality monitoring (Braun et al., 2018), invasive species and pest biology (César De Sá et al., 2017; Große-Stoltenberg et al., 2016; Kislov et al., 2021; Mouta et al., 2023; Vaz et al., 2018), and

agricultural management (Khanal et al., 2020), among others. The rising interests in the application of remote sensing data has been encouraged by the development of data sources with improved spatial and spectral resolution, as well as faster revisit time, allowing for improvements in class discrimination, assessment of fine-scale processes and near real-time monitoring of catastrophic events such as fires and extreme weather events (e.g., Justice et al., 2002).

Machine learning techniques have become predominant in the retrieval of products from satellite imagery for remote sensing analysis, and typically outcompete traditional approaches such as GLM's, making them ideal for modelling complex systems (Atkinson and Tatnall, 1997; LeCun et al., 2015; Olden et al., 2008; Zhou et al., 2023).

Artificial neural networks (ANNs) are among these methods. ANNs extend the concept of a simple artificial neuron to an interconnected network capable of handling highly complex and high-dimensional nonparametric data to extract meaningful patterns, including non-linear relationships and variable interactions (Dragović, 2022; Olden et al., 2008). These algorithms are, therefore, usually seen as more capable than other methods at handling complex ecological datasets (Brosse and Lek, 2000; Olden et al., 2008; Özesmi et al., 2006; Pearson et al., 2002). ANNs date back to the 1940’s, when the concept of the biologically inspired artificial neuron was first described (McCulloch and Pitts, 1943) and became popular after the development of back-propagation training algorithms (Rumelhart et al., 1986). ANNs have since been extensively used in remote sensing (e.g., Atkinson and Tatnall, 1997; Mas and Flores, 2008; Philippopoulos et al., 2023; Wang et al., 2022; Yang et al., 2018; Young et al., 2024) and ecological research (e.g., Kislov et al., 2021; Lek and Guégan, 1999; Olden et al., 2008; Özesmi et al., 2006; Tarroso et al., 2012). The diversity of ANNs has increased over the years with multiple architectures of different complexity (Alzubaidi et al., 2021; LeCun et al., 2015). Convolutional Neural Networks (CNNs) have become a dominant architecture for image analyses, with broad application to remote sensing and ecological research (Brodrick et al., 2019). However, CNNs are typically very large networks, requiring substantial computational resources for training, which often necessitates specialized hardware (Alzubaidi et al., 2021; LeCun et al., 2015). This dependency can limit their accessibility for small scale applications. Additionally, CNNs focus on spatial neighbourhoods, leveraging spatial patterns and edges to detect features within an image. This makes them highly effective for tasks such as image segmentation but less useful when the spectral information dominates, and spatial context is less relevant. Another challenge with CNNs is their reliance on large amounts of training data, which can be a limitation in remote sensing applications. Specifically, hyperspectral datasets relevant to the subjects of interest in landscape-level remote sensing are often scarce or not widely available in public databases (Liu et al., 2022; Song et al., 2019).

A significant portion of remote sensing datasets exists in the form of tabular data, representing features intended for classification in remote sensing imagery, with the expectation that they exhibit distinct spectral signatures. This classification task is commonly performed using regression frameworks and machine learning algorithms, and Artificial Neural Networks excel in this area due to their ability to capture and model complex non-linear patterns in the data (e.g., Landi et al., 2010; Mas and Flores, 2008).

Achieving an optimal network architecture is crucial to minimizing the trade-off between bias and variance, but can be a time consuming process (Geman et al., 1992). To address variability in model predictions, a common approach is to ensemble multiple models (e.g., Araújo et al., 2005; Dietterich, 2000; Sillero et al., 2021). This involves the creation and subsequent integration of multiple models by altering initial conditions, such as through resampling the dataset. Such ensembling methods are common, for example, in ecological research approaches such as distribution modelling (e.g., Liz et al., 2023; Martínez-Freiría et al., 2020). A typical method for neural networks is bagging, which requires bootstrapping the original dataset (Dietterich, 2000). Other resampling techniques, such as repetitions without replacement and k-fold cross-validation, can also be used (Olden et al., 2008). These methods do not require as many replicates, thereby saving processing time while still providing solutions with good generalization (Araújo et al., 2005; Tarroso et al., 2012).

We hereby provide a new method for supervised learning based on an artificial neural network classifier that is implemented in python and named *Spectral Pattern Analysis and Remote-sensing Tool with Artificial Neural Networks* (SpartANN). It provides an easy-to-use interface for training models, allowing different strategies of model replication to achieve good generalizations. Importantly, the application is free-to-use and open source, ensuring reproducibility and is highly adaptable to the needs of individual users. It depends on few packages, ensuring easy installation, and export of simple model output that can be used for predicting. We demonstrate the functioning and flexibility of SpartANN with a cloud cover classification exercise using Sentinel-2 imagery.

2. Methods

SpartANN is written in python and provides an easy interface for training models with Artificial Neural Networks. Although currently there are options for deep learning with artificial neural networks (e.g., Alzubaidi et al., 2021; Liu et al., 2022), SpartANN offers a user-friendly alternative, eliminating the need for complex installation procedures involving multiple library components. Written entirely in Python, it requires only a minimal set of libraries for raster manipulation.

Designed specifically for spatial remote sensing data, SpartANN provides a simple interface to build complex models using just a set of classification locations, labels, and standard raster-format imagery. Additionally, it offers the flexibility to accommodate more advanced use cases by functioning as a Python module, allowing users to integrate it seamlessly into their workflows.

SpartANN provides a versatile Multilayer Perceptron (MLP) framework that can be extended to user-defined complexities, supporting multiple hidden layers with customizable nodes. From simple single-hidden-layer architectures to deep learning structures, SpartANN offers fully connected networks with backpropagation-based learning. It implements a variety of optimization algorithms, including stochastic gradient descent, momentum, RMSprop, Adagrad, and Adam, ensuring efficient training. By default, SpartANN uses the tanh activation function but also supports sigmoid, ReLU, or any user-defined activation function with its corresponding derivative. Fully leveraging the ANN architecture, SpartANN handles a wide range of classification tasks, accommodating binary or continuous inputs and generating single or multiple outputs, depending on the network configuration and the available data.

The strength of SpartANN is the simple interface for associating the tabular data of feature location to raster imagery, extracting the necessary data for training the networks. It requires minimal configurations, which include the necessary indication of input/output data location, intended network architecture, number of repetitions for ensemble and percentage of data reserved for testing purposes. However, parameters can be further configured via python interface. These include the possibility to ensemble multiple network architectures of varying complexity. Besides the ANN implementation, SpartANN offers an interface for simple saving and retrieval of trained models for predictions and model sharing. During the iterative training of the networks, both the network's error and Cohen’s kappa performance metric are reported. When multiple outputs are required, both the training data for the expected outcome and the network's outputs are linearized, and the performance metric is calculated. Training stops when error minimization becomes negligible or when the maximum number of iterations is reached. The best network is selected as the one with the highest product of the training and test Cohen’s kappa values. The trained model can be applied to other imagery, provided the spectral information matches that used during training. Raster predictions generated with SpartANN include detailed metadata, ensuring the reproducibility of results and easy access to each output product. Repetitions and different network architectures are stored as separate bands in the output raster, accompanied by clear and unambiguous descriptions indicating the exact location and context of each product.

SpartANN is available both as a Python module and as a set of command-line tools, offering simple access to model training, prediction, and ensembling for most uses. SpartANN is available in https://github.com/ptarroso/SpartANN

3. Test case

To test the effectiveness of SpartANN, we performed a cloud artifact classification on a Level-1C Sentinel-2 image of tile T29TNF, corresponding to centre-north Portugal, taken in 19th January 2024 (S2A_MSIL1C_20240119T112401_N0510_R037_T29TNF_20240119T132118.SAFE ; Fig. 1). This area was chosen to represent a variety of landscape features (urban, farmland, forest) and water bodies (rivers and ocean), in order to test the applicability of SpartANN in dealing with images representing complex and varied landscapes. Supervised machine-learning approaches tend to outperform threshold-based approaches (e.g., Mei et al., 2017; Zhu et al., 2015) in single-scene cloud classification, and ANNs have been previously shown to be good candidates for cloud detection (Gómez-Chova et al., 2007; Hollstein et al., 2016; Hughes and Hayes, 2014).

We manually digitized 448 points corresponding to five distinct classes: thick/opaque clouds (considering cloud cover which completely obscures the surface below), thin/semi-transparent clouds (cloud cover which allows partial visibility to the surface below), cloud shadows (obscured surface areas caused by cloud cover but not by topography), water (fresh and saltwater) and others (clear unobstructed land surfaces, whether natural or artificial). 48 points corresponded to water bodies, while the remaining classes were represented by 100 points each.
The original Sentinel-2 image was processed in Python using the GDAL library to extract a raster in GeoTIFF format containing 13 raw spectral bands (visible, near-infrared, and shortwave infrared) at a uniform spatial resolution of 10 m. Downscaling of the 20 m and 60 m bands to 10 m resolution was achieved through simple pixel division by factors of 2 and 6, respectively.

SpartANN was trained with the 13 spectral bands and set to output one prediction per class (five outputs), representing the probability of each pixel belonging to the specified class. An ensemble modelling approach was used to account for stochastic variability between model predictions. Three different network configurations were used for five replicates each, producing a total of 15 predictions (Table 1). Learning rate was set to 0.001 and the “Adam” optimization strategy was used (momentum parameters set to 0.9 and 0.999).

For testing the predictions and providing an indication of overfitting, 20% of presence-absence data was set aside. Median and standard deviation values per pixel were calculated across all 15

predictions. Median predictions per class were evaluated by calculating the true positive rate (TPR), false positive rate (FPR), accuracy and recall. Predictions were converted to binary presence/absence format (per class), either by selecting the threshold which maximized TPR and minimized FPR, or the one which maximized both accuracy and recall. Model evaluation was performed in R using the 'terra' and 'ROCR' packages (Hijmans, 2024; Sing et al., 2015). Data and code used for the test case is available in SM 1 and Sentinel-2 image can be downloaded in the Copernicus Data Space Ecosystem (https://dataspace.copernicus.eu/).

Table 1 – Training results from SpartANN for detecting 5 feature classes in a Sentinel-2 image. The network structure is described by the number of neurons per layer, including the input layer (13 neurons), the output layer (5 neurons), and the variable hidden layers. Five repetitions were performed using random subsampling of the training data. The table reports the number of iterations required to minimize the error difference, the best-performing iteration, and the final Sum of Squared Errors for the optimal network. Cohen's kappa statistic, used to evaluate performance and guide early stopping, is provided for the training set, testing set, and their combined product.

Net Structure	Repetition	Stop Iteration	Best Iteration	Error	Train k	Test k	Product
[13, 6, 5]	1	977	940	1.404	0.849	0.808	0.686
	2	682	680	2.812	0.85	0.827	0.702
	3	720	719	2.081	0.836	0.811	0.678
	4	635	635	3.236	0.812	0.846	0.687
	5	683	466	3.004	0.823	0.829	0.682
[13, 8, 6, 5]	1	1026	1026	1.911	0.85	0.866	0.736
	2	1168	1093	2.359	0.84	0.838	0.704
	3	968	444	1.478	0.817	0.863	0.705
	4	1116	1045	2.506	0.842	0.857	0.721
	5	1447	1444	0.516	0.869	0.838	0.728
[13, 10, 8, 6, 5]	1	3960	3681	1.26	0.887	0.868	0.77
	2	3065	2385	2.059	0.884	0.888	0.784
	3	2176	2132	2.284	0.871	0.827	0.72
	4	978	491	2.806	0.861	0.794	0.683
	5	1124	967	2.017	0.813	0.86	0.699

4. Results

Five median probability maps were generated for the target area, one for each class under consideration (Fig.1, SM Fig. 1, SM Fig. 2). The thresholds for the optimal binary prediction were identical for both combinations of evaluation metrics on all classes except cloud shadows and others. Overall model performance was high. Accuracy for the optimal binary predictions ranged between 0.91-0.99 (mean = 0.96, standard deviation (sd) = 0.03), while recall ranged between 0.90-

0.98 (mean = 0.95; sd = 0.03). True and false positive rates ranged between 0.88-0.99 (mean = 0.95; sd = 0.04) and 0.02-0.07 (mean = 0.04; sd = 0.02), respectively (Table 2). Model performance was best for the detection of thick/opaque clouds (Accuracy = TPR = 0.99; Recall = 0.98; FPR = 0.01) and worst for cloud shadows (Accuracy = 0.91; Recall = 0.90; TPR = 0.88; FPR = 0.07) (Table 2).

Table 2: Evaluation metrics for median classification per class. Accuracy, Recall, False Positive Rate (FPR) and True Positive Rate (TPR) are described, as well as thresholds for binarization which either maximize accuracy and recall or maximize TPR and minimize FPR

	Accuracy	Recall	Threshold Acc/Rec	FPR	TPR	Threshold FPR/TPR
Thick clouds	0.990	0.982	0.203	0.020	0.990	0.203
Other	0.980	0.926	0.141	0.046	0.950	0.258
Cloud shadows	0.910	0.902	0.384	0.066	0.880	0.445
Thin clouds	0.940	0.967	0.319	0.026	0.940	0.319
Water	0.979	0.955	0.260	0.048	0.979	0.260

The classification workflow implemented produced fifteen predictions per class, for which the median and standard deviation were calculated. Visual inspection of the median classification allowed the detection of false positives in the prediction for thick clouds, largely caused by white glare produced by some built-up structures. These instances of false positives were largely associated with high standard deviation between model replicates, while true positives largely show agreement between predictions (Fig. 2). Likewise, instances of confusion between classes were found between thick and thin clouds. False positives for cloud shadows were largely associated with topographic shadows (marked as “others” under our classification strategy), while cloud shadows over ocean were largely misclassified as water.

Despite these sources of uncertainty, most of the image was correctly classified, with water bodies being successfully identified (both salt- and freshwater), as were cloud/shadow-free land areas (white built-up areas notwithstanding). The majority of cloud shadows on land were correctly identified. The southern and eastern limits of the study area were correctly classified as a mixture of thin and thick clouds, although areas of cooccurrence between these two types of cover sometimes resulted in misclassification (Fig. 1).

5. Discussion

SpartANN shows promise as a reliable and flexible tool for ANN-based classification of satellite imagery, while being straightforward to implement. It can handle complex image classification structures (i.e., involving multiple classes) as well as binary presence-absence classification, and

performs well even in complex scenarios involving hard to disentangle classes. The ability to generate multi-class probabilistic outputs in a single run of the network represents a significant advantage over methods that produce only one prediction per pixel, particularly for detecting ambiguities in predictions. Another key advantage of multi-model ensembling is the ability to assess the reliability of predictions by evaluating the consensus between replicates, thereby mitigating the effects of stochasticity inherent to any single model. Indeed, while our median prediction identified several instances of false positives for opaque clouds related to built-up areas, these were largely caused by the least complex networks in our ensemble. Misclassification of high-reflectance areas such as urban structures and snow is a common source of error in cloud detection (Foga et al., 2017). Maps of standard deviation, which SpartANN produces by default, allow for quick and efficient detection of these areas of incongruence, and exclusion of poorest-performance replicates when necessary.

Although the cloud classification exercise presented in this work showed good results, it does not have the intention to be used as a replacement for established cloud masking approaches (Mateo-García et al., 2018; Skakun et al., 2022) as its ability to predict clouds in other images was not tested, but rather to demonstrate SpartANN's ability to accurately process image classification scenarios involving multiple outputs. Regardless, the method shows promise as an auxiliary tool to complement cloud masking efforts, as well as a primary tool for processing of higher-level imagery. Like any image classification, special effort must be put into disentangling spectrally similar or mixed classes. Such is the case for thick versus thin clouds, which often occur adjacently in gradients of transparency, and cloud- vs. topographic-shadows, which are spectrally similar but have distinct causes. Adding further records for these classes or relying on ancillary information (such as topography data) may help improve identification of these classes.

Given the wide variety of possible remote sensing applications, SpartANN is built around flexibility and full customization to the specific needs of users. We expect this tool to benefit use-cases requiring continuous (e.g., vegetation cover, soil properties, air quality) as well as categorical outputs (e.g., land cover classification, detection and monitoring of catastrophic events), while providing an intuitive assessment of prediction uncertainty which is crucial for practical applications (e.g., wildlife management, agriculture, forestry). Moreover, SpartANN can be easily extended to retrieve data from different images based on shared location or time-stamps, allowing the construction of comprehensive training datasets from scratch for quick and intuitive application.

CRediT authorship contribution statement

Marco Dinis: Conceptualization, Funding acquisition, Writing – original draft, Writing – review and editing. **Pedro Tarroso:** Conceptualization, Funding acquisition, Methodology, Formal analysis, Supervision, Writing – review and editing.

Acknowledgements

This work was supported by National Funds through FCT – Foundation for Science and Technology (ReNat: Renaturing Iberian native forests from Eucalyptus plantations, REF. 2022.10702.PTDC – doi:10.54499/2022.10702.PTDC). M.D. was supported by FCT (2022.10702.PTDC – doi:10.54499/2022.10702.PTDC). P.T. was supported by FCT (DL57/2016/CP1440/CT0008 – doi:sciproj.ptcris.pt/5012EEC)

Bibliography

Alzubaidi, L., Zhang, J., Humaidi, A.J., Al-Dujaili, A., Duan, Y., Al-Shamma, O., Santamaría, J., Fadhel, M.A., Al-Amidie, M., Farhan, L., 2021. Review of deep learning: concepts, CNN architectures, challenges, applications, future directions, Journal of Big Data. Springer International Publishing. https://doi.org/10.1186/s40537-021-00444-8

Araújo, M.B., Whittaker, R.J., Ladle, R.J., Erhard, M., 2005. Reducing uncertainty in projections of extinction risk from climate change. Glob. Ecol. Biogeogr. 14, 529–538. https://doi.org/10.1111/j.1466-822X.2005.00182.x

Atkinson, P.M., Tatnall, A.R.L., 1997. Introduction neural networks in remote sensing. Int. J. Remote Sens. 18, 699–709. https://doi.org/10.1080/014311697218700

Braun, D., Damm, A., Hein, L., Petchey, O.L., Schaepman, M.E., 2018. Spatio-temporal trends and trade-offs in ecosystem services: An Earth observation based assessment for Switzerland between 2004 and 2014. Ecol. Indic. 89, 828–839. https://doi.org/10.1016/j.ecolind.2017.10.016

Brodrick, P.G., Davies, A.B., Asner, G.P., 2019. Uncovering Ecological Patterns with Convolutional Neural Networks. Trends Ecol. Evol. 34, 734–745. https://doi.org/10.1016/j.tree.2019.03.006

Brosse, S., Lek, S., 2000. Modelling roach (*Rutilus rutilus*) microhabitat using linear and nonlinear techniques. Freshw. Biol. 44, 441–452. https://doi.org/10.1046/j.1365-2427.2000.00580.x

Campos, J.C., Brito, J.C., 2018. Mapping underrepresented land cover heterogeneity in arid regions: The Sahara-Sahel example. ISPRS J. Photogramm. Remote Sens. 146, 211–220. https://doi.org/10.1016/j.isprsjprs.2018.09.012

César De Sá, N., Carvalho, S., Castro, P., Marchante, E., Marchante, H., 2017. Using Landsat Time Series to Understand How Management and Disturbances Influence the Expansion of an Invasive Tree. IEEE J. Sel. Top. Appl. Earth Obs. Remote Sens. 10, 3243–3253. https://doi.org/10.1109/JSTARS.2017.2673761

Dietterich, T.G., 2000. Ensemble Methods in Machine Learning, in: International Workshop on Multiple Classifier Systems. pp. 1–15. https://doi.org/10.1007/3-540-45014-9_1

Dragović, S., 2022. Artificial neural network modeling in environmental radioactivity studies – A review. Sci. Total Environ. 847, 157526. https://doi.org/10.1016/j.scitotenv.2022.157526

Foga, S., Scaramuzza, P.L., Guo, S., Zhu, Z., Dilley, R.D., Beckmann, T., Schmidt, G.L., Dwyer,

J.L., Joseph Hughes, M., Laue, B., 2017. Cloud detection algorithm comparison and validation for operational Landsat data products. Remote Sens. Environ. 194, 379–390. https://doi.org/10.1016/j.rse.2017.03.026

Geman, S., Bienenstock, E., Doursat, R., 1992. Neural Networks and the Bias/Variance Dilemma. Neural Comput. 4, 1–58. https://doi.org/10.1162/neco.1992.4.1.1

Gómez-Chova, L., Camps-Valls, G., Calpe-Maravilla, J., Guanter, L., Moreno, J., 2007. Cloud-screening algorithm for ENVISAT/MERIS multispectral images. IEEE Trans. Geosci. Remote Sens. 45, 4105–4118. https://doi.org/10.1109/TGRS.2007.905312

Große-Stoltenberg, A., Hellmann, C., Werner, C., Oldeland, J., Thiele, J., 2016. Evaluation of continuous VNIR-SWIR spectra versus narrowband hyperspectral indices to discriminate the invasive *Acacia longifolia* within a mediterranean dune ecosystem. Remote Sens. 8. https://doi.org/10.3390/rs8040334

Hijmans, R.J., 2024. terra: Spatial Data Analysis.

Hollstein, A., Segl, K., Guanter, L., Brell, M., Enesco, M., 2016. Ready-to-use methods for the detection of clouds, cirrus, snow, shadow, water and clear sky pixels in Sentinel-2 MSI images. Remote Sens. 8, 1–18. https://doi.org/10.3390/rs8080666

Hughes, M.J., Hayes, D.J., 2014. Automated detection of cloud and cloud shadow in single-date Landsat imagery using neural networks and spatial post-processing. Remote Sens. 6, 4907–4926. https://doi.org/10.3390/rs6064907

Justice, C.O., Giglio, L., Korontzi, S., Owens, J., Morisette, J.T., Roy, D., Descloitres, J., Alleaume, S., Petitcolin, F., Kaufman, Y., 2002. The MODIS fire products. Remote Sens. Environ. 83, 244–262. https://doi.org/10.1016/S0034-4257(02)00076-7

Khanal, S., Kushal, K.C., Fulton, J.P., Shearer, S., Ozkan, E., 2020. Remote sensing in agriculture—accomplishments, limitations, and opportunities. Remote Sens. 12, 1–29. https://doi.org/10.3390/rs12223783

Kislov, D.E., Korznikov, K.A., Altman, J., Vozmishcheva, A.S., Krestov, P. V., 2021. Extending deep learning approaches for forest disturbance segmentation on very high-resolution satellite images. Remote Sens. Ecol. Conserv. 7, 355–368. https://doi.org/10.1002/rse2.194

Landi, A., Piaggi, P., Laurino, M., Menicucci, D., 2010. Artificial neural networks for nonlinear regression and classification. Proc. 2010 10th Int. Conf. Intell. Syst. Des. Appl. ISDA'10 115–120. https://doi.org/10.1109/ISDA.2010.5687280

LeCun, Y., Bengio, Y., Hinton, G., 2015. Deep learning. Nature 521, 436–444. https://doi.org/10.1038/nature14539

Lek, S., Guégan, J.F., 1999. Artificial neural networks as a tool in ecological modelling, an introduction. Ecol. Modell. 120, 65–73. https://doi.org/10.1016/S0304-3800(99)00092-7

Liu, K.H., Yang, M.H., Huang, S.T., Lin, C., 2022. Plant Species Classification Based on Hyperspectral Imaging via a Lightweight Convolutional Neural Network Model. Front. Plant Sci. 13, 13:855660. https://doi.org/10.3389/fpls.2022.855660

Liz, A.V., Rödder, D., Gonçalves, D.V., Velo-Antón, G., Tarroso, P., Geniez, P., Crochet, P.A., Carvalho, S.B., Brito, J.C., 2023. Overlooked species diversity in the hyper-arid Sahara Desert unveiled by dryland-adapted lizards. J. Biogeogr. 50, 101–115. https://doi.org/10.1111/jbi.14510

Martínez-Freiría, F., Freitas, I., Zuffi, M.A.L., Golay, P., Ursenbacher, S., Velo-Antón, G., 2020. Climatic refugia boosted allopatric diversification in Western Mediterranean vipers. J. Biogeogr. 47, 1698–1713. https://doi.org/10.1111/jbi.13861

Mas, J.F., Flores, J.J., 2008. The application of artificial neural networks to the analysis of remotely sensed data. Int. J. Remote Sens. 29, 617–663. https://doi.org/10.1080/01431160701352154

Mateo-García, G., Gómez-Chova, L., Amorós-López, J., Muñoz-Marí, J., Camps-Valls, G., 2018. Multitemporal cloud masking in the Google Earth Engine. Remote Sens. 10, 7–9. https://doi.org/10.3390/rs10071079

McCulloch, W.S., Pitts, W., 1943. A logical calculus of the ideas immanent in nervous activity. Bull. Math. Biophys. 5, 115–133. https://doi.org/10.1007/BF02478259

Mei, L., Vountas, M., Gómez-Chova, L., Rozanov, V., Jäger, M., Lotz, W., Burrows, J.P., Hollmann, R., 2017. A Cloud masking algorithm for the XBAER aerosol retrieval using MERIS data. Remote Sens. Environ. 197, 141–160. https://doi.org/10.1016/j.rse.2016.11.016

Mouta, N., Silva, R., Pinto, E.M., Vaz, A.S., Alonso, J.M., Gonçalves, J.F., Honrado, J., Vicente, J.R., 2023. Sentinel-2 Time Series and Classifier Fusion to Map an Aquatic Invasive Plant Species along a River—The Case of Water-Hyacinth. Remote Sens. 15. https://doi.org/10.3390/rs15133248

Olden, J.D., Lawler, J.J., Poff, N.L., 2008. Machine Learning Methods Without Tears: A Primer for Ecologists. Q. Rev. Biol. 83, 171–193. https://doi.org/10.1086/587826

Özesmi, S.L., Tan, C.O., Özesmi, U., 2006. Methodological issues in building, training, and testing artificial neural networks in ecological applications. Ecol. Modell. 195, 83–93. https://doi.org/10.1016/j.ecolmodel.2005.11.012

Pearson, R.G., Dawson, T.P., Berry, P.M., Harrison, P.A., 2002. SPECIES: A spatial evaluation of climate impact on the envelope of species. Ecol. Modell. 154, 289–300. https://doi.org/10.1016/S0304-3800(02)00056-X

Philippopoulos, K., Pantavou, K., Cartalis, C., Agathangelidis, I., Mavrakou, T., Polydoros, A., Nikolopoulos, G., 2023. A novel artificial neural network methodology to produce high-resolution bioclimatic maps using Earth Observation data: A case study for Cyprus. Sci. Total Environ. 893. https://doi.org/10.1016/j.scitotenv.2023.164734

Rumelhart, D.E., Hinton, G.E., Williams, R.J., 1986. Learning representations by back-propagating errors. Nature 323, 533–536. https://doi.org/10.1038/323533a0

Santos, X., Belliure, J., Gonçalves, J.F., Pausas, J.G., 2022. Resilience of reptiles to megafires. Ecol. Appl. 32, 1–14. https://doi.org/10.1002/eap.2518

Sillero, N., Arenas-Castro, S., Enriquez-Urzelai, U., Vale, C.G., Sousa-Guedes, D., Martínez-Freiría, F., Real, R., Barbosa, A.M., 2021. Want to model a species niche? A step-by-step guideline on correlative ecological niche modelling. Ecol. Modell. 456. https://doi.org/10.1016/j.ecolmodel.2021.109671

Sing, T., Sander, O., Beerenwinkel, N., Lengauer, T., Unterthiner, T., Ernst, F.G.M., 2015. R package 'ROCR' Visualizing the performance of scoring classifiers v1.0-11.

Skakun, S., Wevers, J., Brockmann, C., Doxani, G., Aleksandrov, M., Batič, M., Frantz, D., Gascon, F., Gómez-Chova, L., Hagolle, O., López-Puigdollers, D., Louis, J., Lubej, M., Mateo-García, G., Osman, J., Peressutti, D., Pflug, B., Puc, J., Richter, R., Roger, J.C., Scaramuzza, P., Vermote, E., Vesel, N., Zupanc, A., Žust, L., 2022. Cloud Mask Intercomparison eXercise (CMIX): An evaluation of cloud masking algorithms for Landsat 8 and Sentinel-2. Remote Sens. Environ. 274. https://doi.org/10.1016/j.rse.2022.112990

Song, J., Gao, S., Zhu, Y., Ma, C., 2019. A survey of remote sensing image classification based on CNNs. Big Earth Data 3, 232–254. https://doi.org/10.1080/20964471.2019.1657720

Tarroso, P., Carvalho, S.B., Brito, J.C., 2012. Simapse - simulation maps for ecological niche modelling. Methods Ecol. Evol. 3, 787–791. https://doi.org/10.1111/j.2041-210X.2012.00210.x

Vaz, A.S., Alcaraz-Segura, D., Campos, J.C., Vicente, J.R., Honrado, J.P., 2018. Managing plant invasions through the lens of remote sensing: A review of progress and the way forward. Sci. Total Environ. 642, 1328–1339. https://doi.org/10.1016/j.scitotenv.2018.06.134

Wang, L., Zhang, Y., 2024. Filling GRACE data gap using an innovative transformer-based deep learning approach. Remote Sens. Environ. 315. https://doi.org/10.1016/j.rse.2024.114465

Wang, M., Wong, M.S., Abbas, S., 2022. Tropical Species Classification with Structural Traits Using Handheld Laser Scanning Data. Remote Sens. 14, 1–19. https://doi.org/10.3390/rs14081948

Yang, S., Feng, Q., Liang, T., Liu, B., Zhang, W., Xie, H., 2018. Modeling grassland above-ground biomass based on artificial neural network and remote sensing in the Three-River Headwaters Region. Remote Sens. Environ. 204, 448–455. https://doi.org/10.1016/j.rse.2017.10.011

Young, C.C., Cheng, Y.C., Lee, M.A., Wu, J.H., 2024. Accurate reconstruction of satellite-derived

SST under cloud and cloud-free areas using a physically-informed machine learning approach. Remote Sens. Environ. 313. https://doi.org/10.1016/j.rse.2024.114339
Zhou, X., Yue, Q., Li, K.F., Fishbein, E., Chen, X., Tan, L., Newman, S., Fetzer, E., Yung, Y.L., 2024. Characterizing fire and fire atmospheric states from space using collocated hyperspectral infrared sounding and narrow-band imagery. Remote Sens. Environ. 312. https://doi.org/10.1016/j.rse.2024.114318
Zhou, Z., Qiu, C., Zhang, Y., 2023. A comparative analysis of linear regression, neural networks and random forest regression for predicting air ozone employing soft sensor models. Sci. Rep. 13, 1–23. https://doi.org/10.1038/s41598-023-49899-0
Zhu, Z., Wang, S., Woodcock, C.E., 2015. Improvement and expansion of the Fmask algorithm: Cloud, cloud shadow, and snow detection for Landsats 4-7, 8, and Sentinel 2 images. Remote Sens. Environ. 159, 269–277. https://doi.org/10.1016/j.rse.2014.12.014

Figure 1: Cloud classification performed by SpartANN for a Sentinel-2 image from centre-north Portugal. A: True colour image. B: classified image. Integration of classifications into a single image was performed by assigning each pixel to the class with the highest probability. Study area location in western Europe is represented in the bottom of the figure.

Figure 2: Segment of classified image demonstrating difference in standard deviation between accurate cloud classification and misclassification in built-up areas. A: True colour image. B: Classified image. C: median probability of cloud classification. D: Standard deviation of cloud classification. Purple insets represent areas of accurate cloud classification and red insets represent misclassifications.

Figure 1

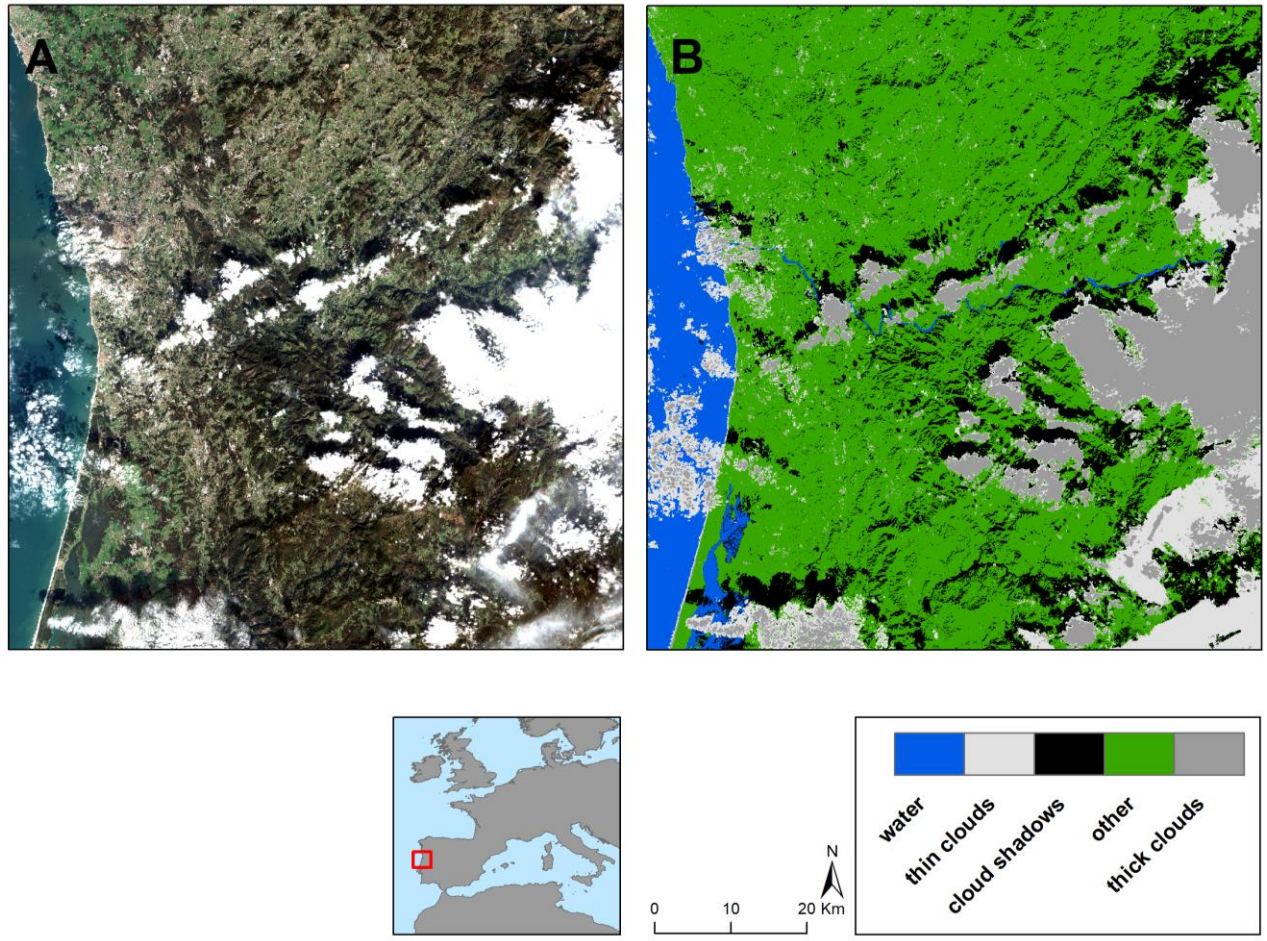
A
B
water
thin clouds
cloud shadows
other
thick clouds
N
0
10
20 Km

Figure 2

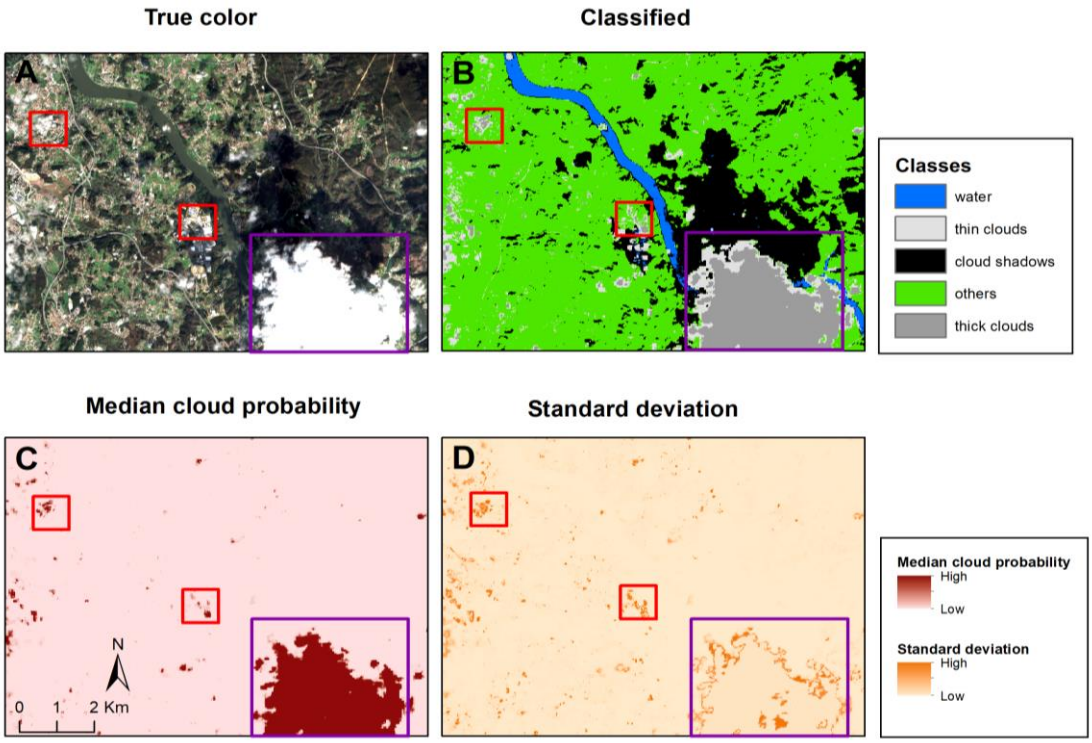
True color
Classified
A
B
Classes
water
thin clouds
cloud shadows
others
thick clouds
Median cloud probability
Standard deviation
C
D
N
0 1 2 Km
Median cloud probability
High
Low
Standard deviation
High
Low

Supplementary materials

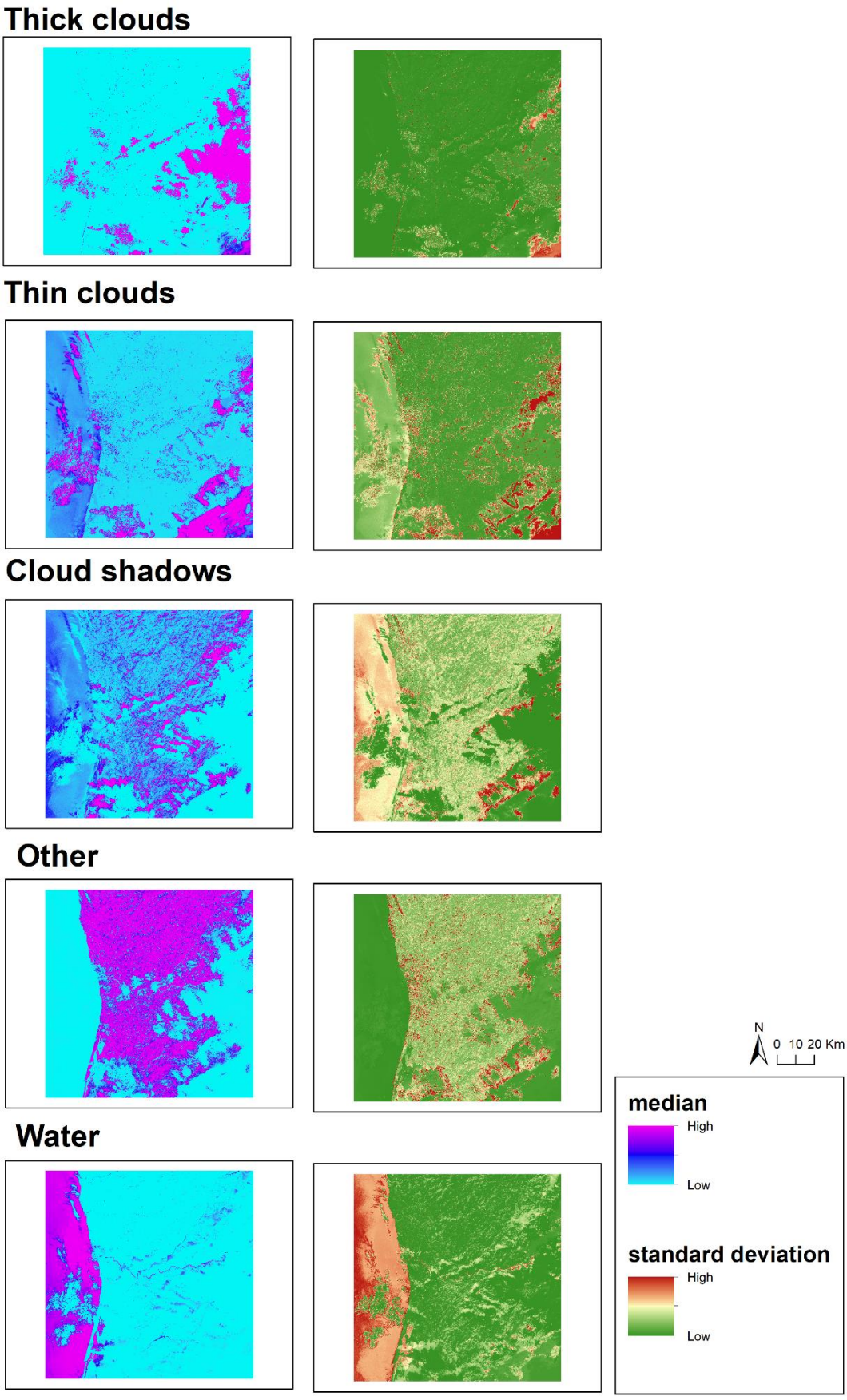

SM Figure 1: Median (left) and standard deviation (right) across 20 replicates for cloud cover classification. Each pair of images corresponds to one class.

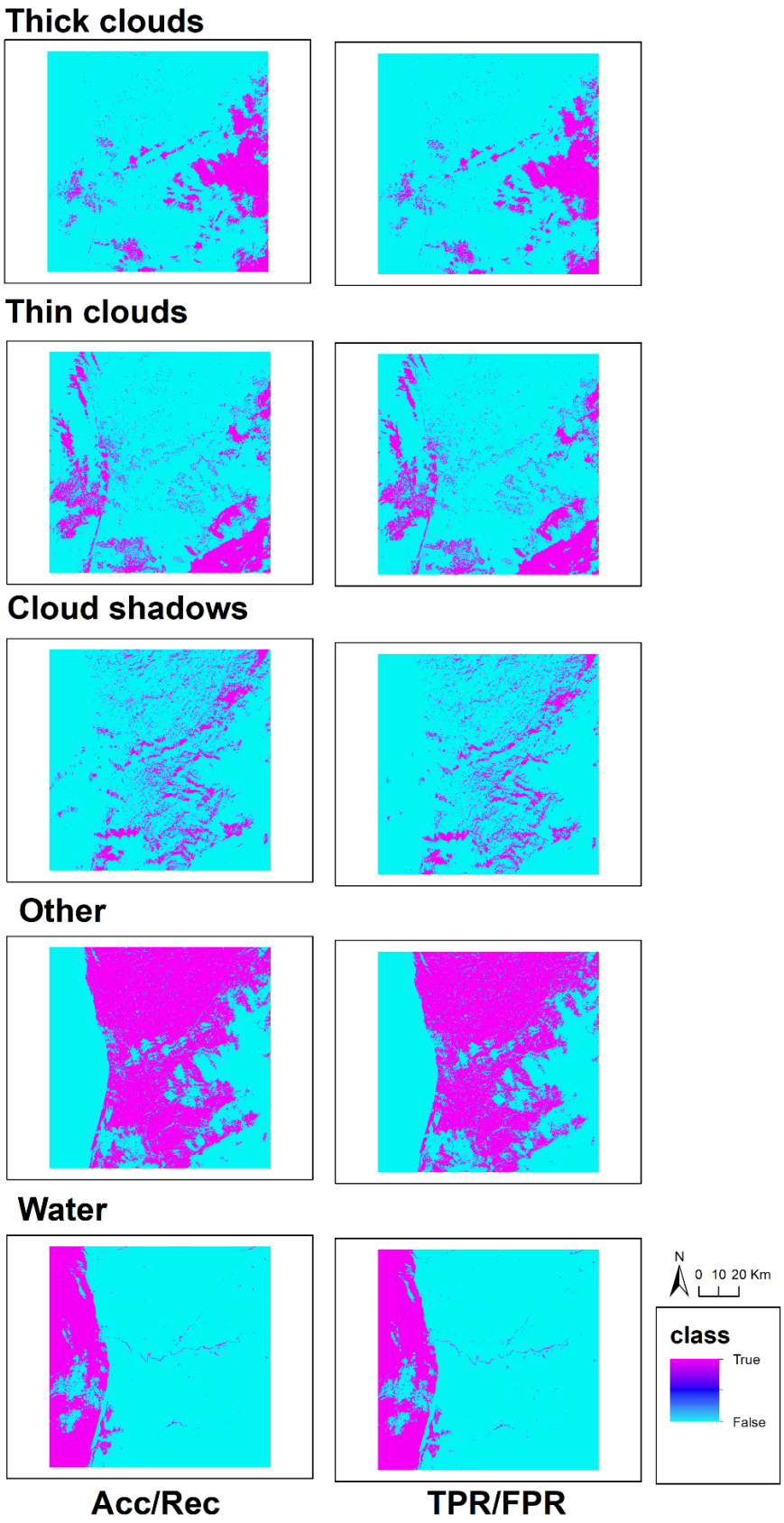

SM Figure 2: Binary cloud cover classification. Each image corresponds to a given class, with true values indicating where the class is predicted to occur and false values where not. Left column represents binary classifications which maximize Accuracy and recall, while right column represents those maximizing True Positive Rate and minimizing False Positive Rate